Switching direction in electric-signal-induced cell migration by cyclic guanosine monophosphate and phosphatidylinositol signaling

Masayuki J. Sato[a,b], Hidekazu Kuwayama[a,1], Wouter N. van Egmond[c], Airi L. K. Takayama[a], Hiroaki Takagi[a,b,2], Peter J. M. van Haastert[c], Toshio Yanagida[a], and Masahiro Ueda[a,b,3]

[a]Laboratories for Nanobiology, Graduate School of Frontier Biosciences, Osaka University, 1-3 Yamadaoka, Suita, Osaka 565-0871, Japan; [b]Core Research for Evolutional Science and Technology, Japan Science and Technology Agency, 1-3 Yamadaoka, Suita, Osaka 565-0871, Japan; [c]Department of Molecular Cell Biology, University of Groningen, 9751 NN, Haren, The Netherlands

Edited by Peter N. Devreotes, Johns Hopkins University School of Medicine, Baltimore, MD, and approved February 24, 2009 (received for review October 7, 2008)

Switching between attractive and repulsive migration in cell movement in response to extracellular guidance cues has been found in various cell types and is an important cellular function for translocation during cellular and developmental processes. Here we show that the preferential direction of migration during electrotaxis in *Dictyostelium* cells can be reversed by genetically modulating both guanylyl cyclases (GCases) and the cyclic guanosine monophosphate (cGMP)-binding protein C (GbpC) in combination with the inhibition of phosphatidylinositol-3-OH kinases (PI3Ks). The PI3K-dependent pathway is involved in cathode-directed migration under a direct-current electric field. The catalytic domains of soluble GCase (sGC) and GbpC also mediate cathode-directed signaling via cGMP, whereas the N-terminal domain of sGC mediates anode-directed signaling in conjunction with both the inhibition of PI3Ks and cGMP production. These observations provide an identification of the genes required for directional switching in electrotaxis and suggest that a parallel processing of electric signals, in which multiple-signaling pathways act to bias cell movement toward the cathode or anode, is used to determine the direction of migration.

cGMP | chemotaxis | electrotaxis | PI3K

Directional cell migration of eukaryotic cells in response to external guidance cues plays crucial roles in many physiological phenomena, such as embryogenesis, neurogenesis, immune response, wound healing, and the regeneration of multicellular organisms, as well as in tactic responses by unicellular organisms (1). Clarifying the molecular basis for determining migration direction is an important topic in cell and developmental biology. Cells can exhibit attractive and repulsive migrations in response to the same external signals. For example, in the chemotactic responses of neuronal cells, growth cones exhibit a repulsive response to a chemotactic signal, but in the presence of membrane-permeable analogs of cyclic nucleotides they exhibit an attractive response (2). Furthermore, investigations of the mechanism underlying reversal in migration direction have revealed that the ratio between intracellular cAMP and cyclic guanosine monophosphate (cGMP) regulates Ca^{2+} channels that are responsible for the directional selection of migration (3). In the case of chemotaxis in *Dictyostelium discoideum*, cells exhibit attraction toward the source of the extracellular chemoattractant cAMP but repulsion from the source of the chemorepellent cAMP analog 8CPT-cAMP (4). Chemoattractants induce activation of phosphoinositide-3-kinases (PI3Ks) and phospholipase C (PLC) at the cell surface with the higher cAMP gradient, leading to localized accumulation and depletion of phosphatidylinositol 3,4,5-trisphosphate [PtdIns(3,4,5)P_3] and phosphatidylinositol 4,5-biphosphate [PtdIns(4,5)P_2], respectively, which induces pseudopod formation directionally toward the chemoattractant source. On the other hand, chemorepellent gradients induce localized inhibition of PLC, leading to localized accumulation of PtdIns(4,5)P_2. This chemorepellent-elicited reaction is opposite that of chemoattractant-elicited ones, meaning that the polarized localization of the PtdIns lipids is reversed, leading to repulsive migration from the chemorepellent. Thus, studies of directional switching in response to external signals have been useful to clarify the molecular mechanisms underlying the direction of migration.

As with chemotaxis, evidence that electrotaxis plays important roles in many physiological phenomena is accumulating (5–9). In electrotaxis, cells move with a directional preference toward the cathode or anode under direct-current electric fields (dcEFs) (5–9). The preferential direction of migration during electrotaxis varies among cell types and under different experimental conditions. For example, corneal rat epithelial cells, human keratinocytes, osteoblasts, rat prostate cancer cells, lymphocyte, and *Xenopus* neurons migrate toward the cathode, whereas corneal stromal fibroblasts, osteoclasts, human granulocyte, and macrophage migrate toward the anode. Even in the same cell type, cells derived from different species exhibit opposite migration direction in dcEFs; bovine vascular endothelial cells migrate toward the cathode, whereas human vascular endothelial cells migrate toward the anode (10, 11). Furthermore, lens epithelial cells change their migration direction depending on the applied electric field strength (12). However, despite the mechanistic importance regarding the coupling between gradient sensing and directional cell migration, the molecules responsible for selecting migration direction in electrotaxis have not been identified.

To investigate the molecular mechanisms underlying the determination of migration direction in electrotaxis, we here used cellular slime mold *D. discoideum*. *Dictyostelium* cells present a well-established model for elucidating the mechanisms and regulation of amoeboid movements (13–17). Their chemotactic responses have been extensively studied at the molecular and cellular levels, which has resulted in the identification of multiple and parallel chemotactic signaling pathways (18–21). Because *Dictyostelium* cells exhibit strong electrotaxis, they are

Author contributions: M.J.S., P.J.M.v.H., and M.U. designed research; M.J.S. and A.L.K.T. performed research; H.K. and W.N.v.E. contributed new reagents/analytic tools; M.J.S. and H.T. analyzed data; and M.J.S., P.J.M.v.H., T.Y., and M.U. wrote the paper.

The authors declare no conflict of interest.

This article is a PNAS Direct Submission.

[1]Present address: Graduate School of Life and Environmental Sciences, University of Tsukuba, 1-1-1 Tennoudai, Tsukuba, Ibaraki 305-8572, Japan.

[2]Present address: Department of Physics, Nara Medical University, 840 Shijocho, Kashihara City, Nara 634-8521, Japan.

[3]To whom correspondence should be addressed. E-mail: ueda@phys1.med.osaka-u.ac.jp.

This article contains supporting information online at www.pnas.org/cgi/content/full/0809974106/DCSupplemental.

also useful for studying the mechanism of this process (22, 23). Previous reports revealed that upstream components of chemotactic signaling pathways such as cAMP receptor 1 and its coupled heterotrimeric G proteins are not essential for electrotaxis (in contrast to chemotaxis) (22), although whether downstream components are involved in electrotaxis has not been examined. Here we found that chemotaxis-deficient mutant cells, which have defects in their guanylyl cyclase (GCase)-dependent signaling pathway, exhibited reversed migration in electrotaxis. We further confirmed that simultaneous suppression of GCase and PI3K activities caused switching in the preferential direction of migration from the cathode to the anode in response to the same electric signals. These observations provide identification of the genes required for directional switching in electrotaxis.

Results

Defects of KI Mutant Cells in Electrotaxis. First, we examined the effects of electric signals on a series of mutant cells called KI mutants, originally isolated as chemotaxis-deficient mutants by means of chemical mutagenesis (24). We used 3 types of mutants—KI-5, KI-8, and KI-10—for electrotactic assays. Biochemical characterization of these mutants during chemotactic responses revealed that KI-8 cells have virtually no GCase activity, KI-10 cells have basal GCase activity but are not activated by chemoattractants, and KI-5 cells exhibit relatively normal chemoattractant-mediated GCase activation (25, 26). In the absence of an electric field, these mutant cells and WT cells moved randomly in all directions with a migration velocity between ≈6 and 26 μm·min^{-1} (Table S1). Upon electrical stimulation, WT cells moved toward the cathode. This movement became obvious by gradually increasing the electric field strength. At 10 V·cm^{-1}, the cells' maximum electrotactic efficiency was reached (Fig. 1 *A* and *B* and Movie S1). KI-5 cells moved efficiently toward the cathode at 10 V·cm^{-1} showing no defects in electrotaxis (Fig. 1 *C* and *D*). Impaired responses to electric stimulation were clearly observed in the other KI mutant cells. KI-8 cells moved toward the anode, a direction opposite of WT cells at the same dcEF strength (Fig. 1 *E* and *F* and Movie S2). KI-10 cells moved in random directions (Fig. 1 *G* and *H*). To examine the effects of electric signals on cell motility, we analyzed quantitatively the motile properties of cells as summarized in Table S1. The preferential direction and migration speed depended on the mutant types but not on the dcEF strength (Fig. 1 *I* and *J*). Reversal of preferential direction was constantly observed in KI-8 cells between 1 and 10 V·cm^{-1}. Thus, severe defects in directional movement during electrotaxis were observed in KI-8 and KI-10 but not in KI-5, indicating that the molecular mechanisms for electrotaxis are shared in part with those of chemotaxis. Mutant type-specific directionality in KI mutants during electrotaxis suggests that GCase activity is involved in determining the migration direction. We should note that the responsible mutation(s) in KI mutants has not been identified genetically (24).

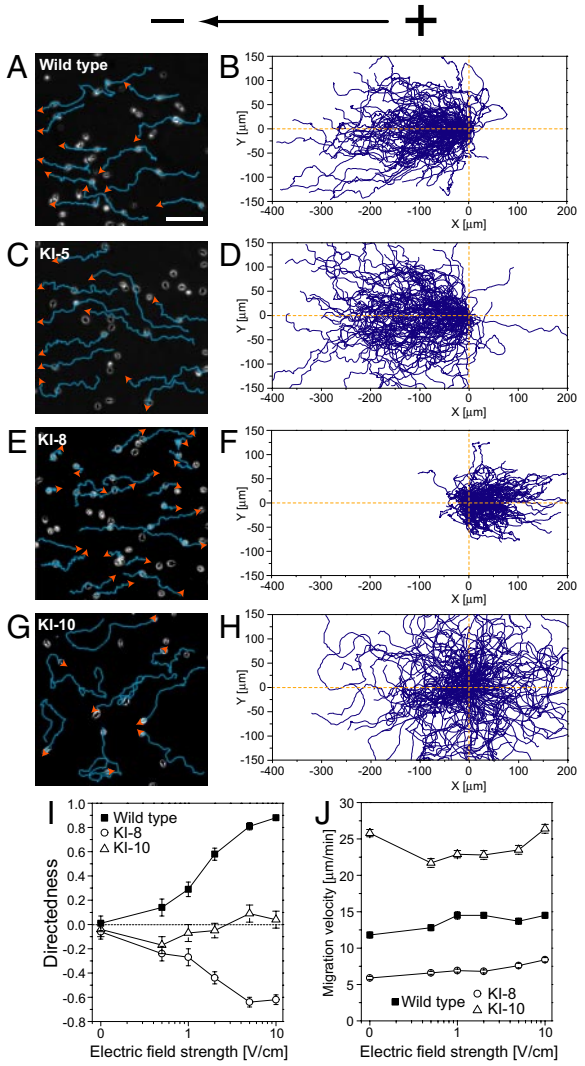

Fig. 1. Reversal of directional preference during electrotaxis in KI-8, a particular chemotaxis-deficient mutant. (*A–H*) Migration of WT cells (*A* and *B*) and the mutants KI-5 (*C* and *D*), KI-8 (*E* and *F*), and KI-10 (*G* and *H*) under a dcEF (10 V·cm^{-1}) in which WT and the KI-5 mutant migrated toward the cathode. The KI-8 mutant moved toward the anode. The KI-10 mutant migrated in random directions. Blue lines and orange arrows represent the cell trajectory and its direction of migration, respectively. (*B*, *D*, *F*, and *H*) Cell trajectories in 10 V·cm^{-1}. The starting points for cell migration were at the origin. (*I*) Dependence of directedness on the dcEF strength. (*J*) Although migration velocity was specific for cell type, velocity had minimal dependence on electric field strength. Data (mean ± SEM) for each cell type were quantified from 7–9 independent experiments. (Scale bar, 100 μm.)

Switching Direction by Simultaneous Inhibition of GCase and PI3K-Mediated Signaling Pathways. To test directly whether the GCase-dependent signaling pathway is involved in the electrotaxis of *Dictyostelium* cells, we next examined the effects of genetically disrupting GCases and the cGMP-binding protein on the electrotactic response (Fig. 2). In *Dictyostelium* cells, 2 types of GCases—GCase A (GCA) and soluble GCase (sGC)—have been identified as responsible for all cGMP production in cells (27). cGMP-binding protein C (GbpC) is the major binding target for intracellular cGMP and transmits cGMP signals, which are responsible for the regulation of myosin filament formation on the side and at the tail end of *Dictyostelium* cells (28, 29). Thus, both GCases and GbpC are the upstream and downstream molecules of cGMP, respectively. On electric stimulation (10 V·cm^{-1}), both *gca*$^{-}$/*sgc*$^{-}$ (*gc*-null) and *gbpC*-null cells exhibited attenuated directional migration toward the cathode, indicating that the GCase-dependent signaling pathway plays an important role in cathode-directed electrotaxis (Fig. 2 *A*, *B*, and *E*). Consistent with this observation, the electrotactic efficiency of *gbpA*$^{-}$/*gbpB*$^{-}$ cells, which lack the degradation activities of intracellular cGMP, was almost the same as that of WT cells (Fig. 2 *E* and *F*) (28, 29). Thus, the GCase-dependent cGMP signaling mediates cathode-directed electrotaxis. However, in contrast to KI-8 cells, the *gc*-null and *gbpC*-null cells were still able to move toward the cathode, showing no reversal of preferential direction. Therefore, the GCase-dependent pathway is not solely responsible for cathode-directed electrotaxis, indicating that

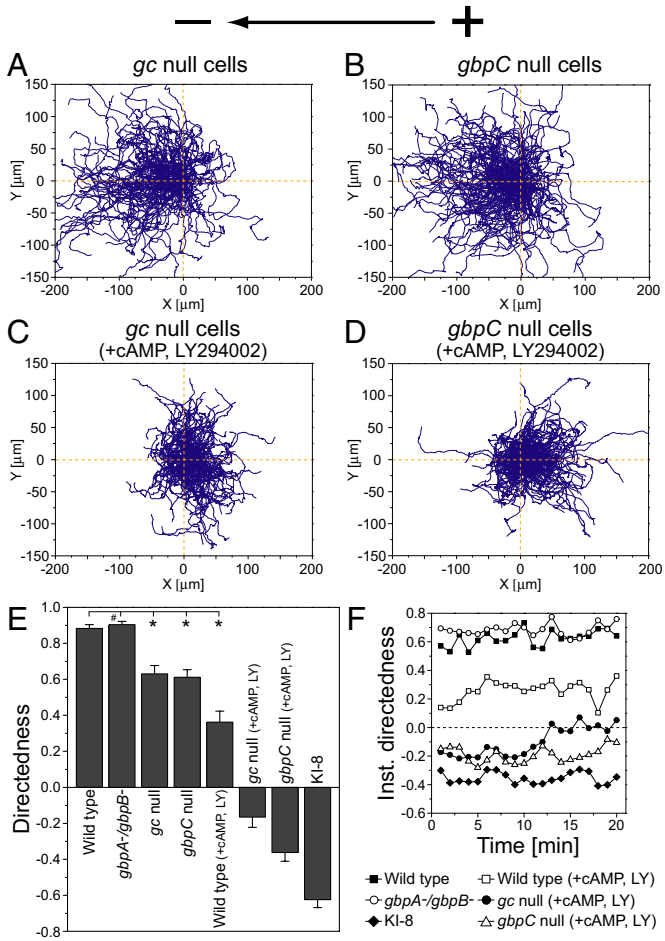

Fig. 2. Switching migration direction during electrotaxis by simultaneous inhibition of GCase and PI3Ks activities. (*A* and *B*) Cell trajectories of *gc*-null (*A*) and *gbpC*-null (*B*) cells at 10 V·cm^{-1}. (*C* and *D*) Reversal of preferential direction was observed in *gc*-null (*C*) and *gbpC*-null (*D*) cells in the presence of 60 μM LY294002, a PI3K inhibitor, and 1 μM cAMP at 10 V·cm^{-1}. (*E*) Directedness at 10 V·cm^{-1}. Migration direction was reversed only when the activity of cGMP- and PI3K-dependent pathways was suppressed simultaneously. *, $P < 0.01$ compared with WT cells at 10 V·cm^{-1}; #, no statistical significance, unpaired Student's *t* test. (*F*) Time course of directedness (instantaneous directedness) at 10 V·cm^{-1} in which directedness of cells was obtained in 1-min intervals. Data (mean ± SEM) for each cell type were quantified from 8–11 independent experiments.

additional GCase-independent pathways are involved in cathode-directed electrotaxis.

PI3Ks comprise one candidate for the GCase-independent signaling pathways because their involvement in electrotaxis has been revealed in other cell types (9, 11, 30). In *Dictyostelium*, PI3K2 is highly localized at the leading edge of moving cells. On the membranes of these moving cells, PI3K2 catalyses the production of PtdIns(3,4,5)P_3, a molecule key in regulating the localized activation of actin polymerization via interaction with pleckstrin homology (PH)-domain-containing proteins such as Akt/PKB (19–21). To test the possible involvement of PI3Ks in electrotaxis, we examined the effects of a PI3K inhibitor, LY294002, on the electrotaxis of WT, *gc*-null, and *gbpC*-null cells (Fig. 2 *C–F*). Because treatment with 60 μM LY294002 strongly inhibited basal cell migration (see Table S1), we added 1 μM cAMP to the medium to restore the basal speed of cell movement (31, 32). In WT cells, treatment with 1 μM cAMP alone enhanced the cathode-directed electrotaxis (Table S1), whereas the addition of 60 μM LY294002 with 1 μM cAMP strongly attenuated the cathode-directed electrotaxis (Fig. 2 *E* and *F*), thus demonstrating the involvement of PI3Ks in electrotaxis toward the cathode. In the same medium conditions, *gc*-null and *gbpC*-null cells exhibited anode-directed electrotaxis opposite that of WT cells (Fig. 2 *C–F* and Movie S3). These results reveal that simultaneous inhibition of GCase- and PI3K-mediated signaling pathways is required to reverse migration direction. The anodal electrotaxis under the simultaneous inhibition suggests that GCase- and PI3K-independent pathways are involved in biasing cell migration toward the anode.

Opposite Function of sGC Subdomains in the Determination of Migration Direction. sGC contains an N-terminal domain, which shows no homology to any other known protein sequence, and a catalytic domain that have distinct functions during chemotaxis (18, 33). In chemotaxis, the N-terminal domain mediates the "front" signal via interaction with the actin cytoskeleton at the leading-edge pseudopod, whereas the catalytic domain mediates the "rear" signal via cGMP-dependent myosin activation at the tail (18, 33). To examine whether both domains of sGC have some functional differences in electrotaxis, we further studied *gc*-null cells expressing either sGC with an inactivated catalytic domain (sGCΔCat) or sGC with a deleted N-terminal domain (sGCΔN) (Fig. 3). Although sGCΔCat does not produce cGMP, it can mediate the front signal for chemotaxis (18, 33). On the contrary, sGCΔN shows WT-like cGMP production and can mediate the rear signals for chemotaxis (18, 33). In a dcEF, *gc*-null cells expressing sGCΔN (*gc*-null/sGCΔN) exhibited full recovery of cathode-directed electrotaxis with an efficiency similar to that of WT cells, whereas *gc*-null cells expressing sGCΔCat (*gc*-null/sGCΔCat) exhibited attenuated cathode-directed electrotaxis (Fig. 3 *A*, *B*, and *G*). The directedness of *gc*-null/sGCΔN and *gc*-null/sGCΔCat cells was 0.83 units and 0.32 units, respectively, which is larger and smaller than the directedness of parental *gc*-null cells (0.63 units), respectively. That is, expression of the catalytic domain (sGCΔN) and the N-terminal domain (sGCΔCat) in *gc*-null cells caused enhancement and inhibition of the cathode-directed electrotaxis, respectively. These results confirm that the catalytic product cGMP mediates cathode-directed signaling in electrotaxis.

To further examine the roles of the catalytic and N-terminal domains of sGC in electrotaxis, other cathode-directed signaling pathways were inhibited by adding cAMP and LY294002. Treatment of cAMP alone to *gc*-null/sGCΔN and *gc*-null/sGCΔCat cells had inhibitory effects on the cathode-directed electrotaxis (Fig. 3 *C* and *D*). Directedness decreased incrementally by ≈0.4–0.5 units for both cell types (Fig. 3*G*), meaning that cAMP constantly affects the background phenotype. In this medium condition, the expression of sGCΔN and sGCΔCat biased *gc*-null cells toward the cathode and anode, respectively. When further treated with 60 μM LY294002 to inhibit PI3K-dependent cathode-directed signaling, directional switching toward the anode was clearly observed in *gc*-null/sGCΔCat cells but not in *gc*-null/sGCΔN cells (Fig. 3 *E* and *F*). The respective directedness of *gc*-null/sGCΔN and *gc*-null/sGCΔCat cells was 0.01 and −0.67 units in the presence of cAMP and the PI3K inhibitor, which is larger and smaller, respectively, than that of parent *gc*-null cells (−0.17) (Figs. 2*E* and 3*G* and Table S1). That is, expression of the catalytic and N-terminal domains of sGC in *gc*-null cells consistently caused the cathode-directed and anode-directed bias in electrotaxis, respectively, even when the cathode-directed signaling was successively inhibited by cAMP and the PI3K inhibitor. The anode-directed electrotaxis of *gc*-null/sGCΔCat became more obvious and stable with time than the electrotaxis of *gc*-null cells, showing an enhancement of anode-directed signaling (Figs. 2*F* and 3*H* and Movie S4). Thus, sGC has competing functions in electrotaxis in which the catalytic and N-terminal domains of sGC mediate electrotactic signals to bias

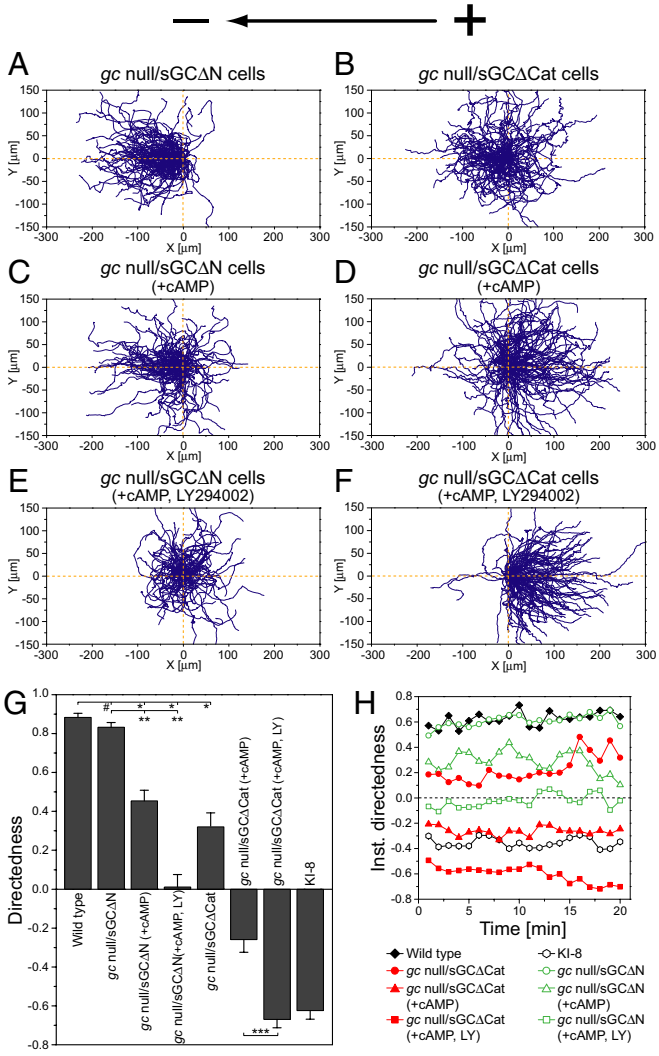

Fig. 3. Opposite function of GCase subdomains to determine migration direction during electrotaxis. (*A* and *B*) Control. (*C* and *D*) cAMP at 1 μM. (*E* and *F*) cAMP at 1 μM and LY294002, a PI3K inhibitor, at 60 μM. (*A–F*) Cell trajectories of *gc*-null cells expressing sGCΔN (*gc*-null/sGCΔN) (*A*, *C*, and *E*) or sGCΔCat (*gc*-null/sGCΔCat) (*B*, *D*, and *F*) at 10 V·cm^{-1}. Expression of sGCΔN or sGCΔCat into *gc*-null cells consistently caused the cathode-directed and anode-directed bias in electrotaxis, respectively, regardless of whether cAMP and the PI3K inhibitor were present or not. (*G*) A summary of directedness. *, $P < 0.01$ compared with WT cells at 10 V·cm^{-1}. **, $P < 0.01$ compared with *gc*-null/sGCΔN cells at 10 V·cm^{-1}. ***, $P < 0.01$ compared with *gc*-null/sGCΔCat cells treated with 1 μM cAMP at 10 V·cm^{-1}. #, no statistical significance, unpaired Student's *t* test. (*H*) Time course of directedness (instantaneous directedness) obtained in 1-min intervals at 10 V·cm^{-1}. Data (mean ± SEM) for each cell type was quantified from 8–11 independent experiments.

cell migrations toward the cathode and anode, respectively. Because WT sGC, which has both domains, mediates cathode-directed signaling in electrotaxis (Fig. 2*A*), the catalytic domain dominates the N-terminal domain in WT sGC, and thus the anode-directed signaling by the N-terminal domain is somehow inhibited.

Extracellular cAMP had bidirectional effects on electrotaxis in a cell-type-dependent manner. cAMP addition to the medium enhanced the cathode-directed electrotaxis in WT cells but attenuated it in *gc*-null/sGCΔN and *gc*-null/sGCΔCat cells (Fig. 3 and Table S1). Because cAMP is charged negatively, this finding suggests the possibility that cAMP addition to the medium may cause chemotaxis toward the anode through a gradient generation of cAMP caused by the applied dcEFs (34),

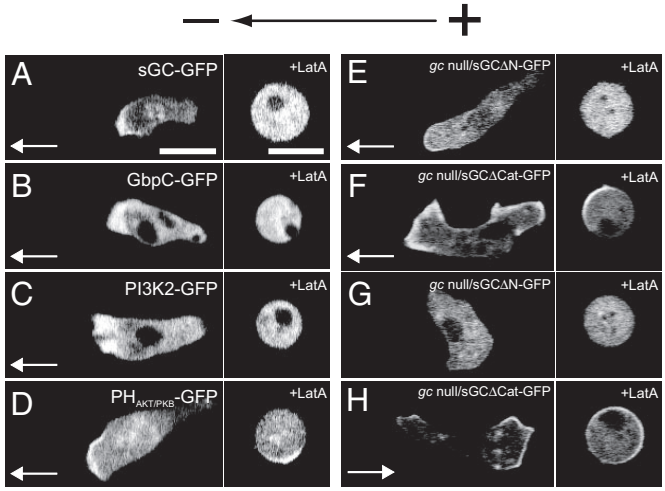

Fig. 4. Intracellular localization of signaling molecules responsible for electrotaxis under a dcEF. (*A–F*) Confocal images of cells expressing sGC-GFP (*A*), GbpC-GFP (*B*), PI3K2-GFP (*C*), PH$_{Akt/PKB}$-GFP (*D*), sGCΔN-GFP (*E*), and sGCΔCat-GFP (*F*) at 10 V·cm^{-1} in the absence of cAMP and LY294002, a PI3K inhibitor. In this condition, cells exhibited cathode-directed electrotaxis. (*G* and *H*) Confocal images of cells expressing sGCΔN-GFP (*G*) and sGCΔCat-GFP (*H*) at 10 V·cm^{-1} in the presence of 1 μM cAMP and 60 μM LY294002. Migration directions are represented by white arrows. (*A–D*) No treatment Latrunculin A. (*E–H*) Presence of Latrunculin A at 5 μM. (Scale bar, 10 μm.)

which may at least account for the cAMP-dependent attenuation of the cathode-directed electrotaxis. However, cross-current fluid flow experiments, in which the medium including 1 μM cAMP and 60 μM LY294002 was perfused continuously across the chamber in the direction perpendicular to the electric fields, revealed no obvious changes in the migration direction toward the anode in *gc*-null/sGCΔCat cells, confirming no effect by possible field-induced artifacts such as chemical gradients. In chemotaxis, it has been revealed that PI3K- and GCase-mediated signaling pathways are modulated by extracellular cAMP stimulation (18–21). Similarly, the bidirectional effects of cAMP in electrotaxis may be due to cAMP-dependent modulation of the intracellular dynamics of multiple-signaling pathways.

Intracellular Localization of Electrotactic Signaling Components During Electrotaxis. We next examined the intracellular localization of sGC, GbpC, sGCΔN, and sGCΔCat for the GCase-mediated signaling pathway and the localization of PI3K2 and the PH domain of Akt/PKB for the PI3K-mediated signaling pathway during electrotaxis under a dcEF (10 V·cm^{-1}) by using GFP (sGC-GFP, GbpC-GFP, sGCΔN-GFP, sGCΔCat-GFP, PI3K2-GFP, and PH$_{Akt/PKB}$-GFP, respectively). PH$_{Akt/PKB}$-GFP is an indicator for PtdIns(3,4,5)P_3, which is the catalytic product of PI3Ks on the membrane. In the condition in which cells exhibit cathode-directed electrotaxis, these proteins were all localized at the leading edge of cells migrating toward the cathode (Fig. 4 *A–E*) except for sGCΔCat-GFP, which was often localized both at the leading edge and the tail end of the migrating cells (Fig. 4*F*). These distributions resemble those observed in chemotactic cells under cAMP gradients (18–21, 35). The presence of sGC, GbpC, PI3K, and PIP_3 in the pseudopod could stabilize the pseudopod, thereby allowing the cell to preferentially migrate toward the cathode during electrotaxis. Bipolar distribution of sGCΔCat-GFP at the leading edge and tail end of the migrating cells is consistent with the less-effective cathode-directed electrotaxis seen in *gc*-null/sGCΔCat cells.

In the presence of 1 μM cAMP and 60 μM LY294002, which cause anode-directed electrotaxis in *gc*-null/sGCΔCat cells, sGCΔCat-GFP was localized dominantly at the anode-directed

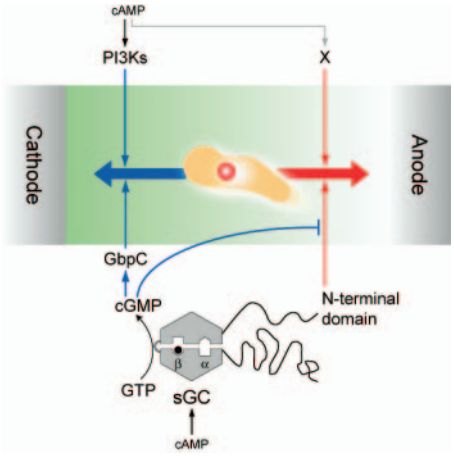

Fig. 5. Model for directional switching in electrotaxis. Multiple-signaling pathways mediate electrotactic signals to bias migration toward the cathode and anode. PI3Ks and the catalytic domain of sGC with GbpC are involved in cathode-directed migration, whereas the N-terminal domain of sGC and unidentified cAMP-activated pathways (X) mediate anode-directed migration. Migration direction is determined by a tug-of-war-like mechanism between the multiple-signaling pathways. The sGC-dependent pathways can be switched between cathode-directed and anode-directed signaling through intracellular cGMP levels.

pseudopod, whereas sGCΔN-GFP was observed in the cytosol with no polarized localization on the membrane (Fig. 4 *G* and *H*). These results suggest that the N-terminal domain of sGC mediates anode-directed signaling by localizing dominantly to the pseudopod facing the anode. Because WT sGC-GFP was localized at the cathode-directed pseudopod (Fig. 4*A*), the N-terminal domain-dependent localization at the pseudopod facing the anode was somehow inhibited in WT sGC.

When cells were treated with Latrunculin A (5 μM), which is an F-actin-depolymerizing reagent, the distinctive localization of these signaling molecules was lost, instead of being random, with respect to the direction of the electric field (10 V·cm^{-1}) (Fig. 3 *B*, *D*, *F*, *H*). Both $PH_{Akt/PKB}$-GFP and sGCΔCat-GFP were localized on the membrane in an F-actin-independent manner, but their localization was not polarized under a dcEF. These observations indicate that signaling molecules of the GCase- and PI3K-mediated signaling pathways are polarized through actin-dependent localization.

Discussion

The results we report here identify genes required to determine migration direction in electrotaxis and show that the GCase- and PI3K-dependent signaling pathways work to bias cell movements in electrotaxis. Similarities and differences in the molecular mechanisms between electrotaxis and chemotaxis are discussed below. Furthermore, we propose a mechanism for switching the direction in electrotaxis, in which parallel processing of electric signals by multiple pathways determine the migration direction toward the cathode or anode (Fig. 5).

Previous reports have revealed that chemotaxis in *Dictyostelium* cells is mediated by PI3K-, PLA2-, and GCase-dependent signaling pathways (18–21, 36, 37). Simultaneous inhibition of these pathways abolishes chemotactic movements completely, whereas functional signaling in either one of these multiple pathways can restore chemotaxis at least in part, suggesting that these pathways work independently (18). Similar to chemotaxis, multiple-signaling pathways work in parallel for electrotaxis to reorient cells directionally toward the cathode or anode (Fig. 5). Both the GCase- and PI3K-dependent signaling pathways are involved in cathode-directed electrotaxis. Suppression of either GCase- or PI3K-dependent signaling partially decreased the electrotactic efficiency (Fig. 2). Molecular components of the GCase- and PI3K-dependent signaling pathways localized at the leading edge of migrating cells during electrotaxis in an actin-dependent manner (Fig. 4). Similar results have been observed in chemotactic cells under chemoattractant gradients in which a distinctive localization of signaling components at the leading edge has been implicated to enhance chemotactic efficiency (20, 35). These results suggest functional sharing of intracellular signaling components for directional cell migration between chemotaxis and electrotaxis.

Nevertheless, there exist significant differences between electrotaxis and chemotaxis. First, although F-actin-independent localization of PtdIns(3,4,5)P_3 on the membrane facing the chemoattractant source is one key signaling event in chemotaxis (20), no localization of PtdIns(3,4,5)P_3 was observed under a dcEF when the actin polymerization was inhibited (Fig. 4). This finding indicates that the PI3K-dependent signaling pathway mediates electrotactic signals in an actin-dependent manner. Because PI3K activity is regulated by a feedback mechanism through a Ras/PI3K/F-actin circuit (20, 32), electric signals may affect some components of this feedback circuit. Second, sGC is involved in both chemotaxis and electrotaxis but in different ways. For example, expression of sGCΔCat in *gc*-null cells can partly restore chemotaxis, but expression of sGCΔN is not sufficient for chemotaxis (18). However, the converse applies to electrotaxis, where *gc*-null/sGCΔCat cells cannot restore effective cathode-directed electrotaxis but *gc*-null/sGCΔN cells can (Fig. 3). Roles of the N-terminal and catalytic domains of sGC in electrotaxis are discussed below with a proposed mechanism (Fig. 5). Additionally, the behaviors of electrotactic cells sometimes depended on the application time of the electric fields. WT and *gc*-null/sGCΔCat cells exhibited electrotaxis continuously toward the cathode and anode, respectively, whereas *gc*-null and *gbpC*-null cells gradually became random during electric field application (Figs. 2*F* and 3*H*). Such stimulation-time-dependent directionality has not been observed in chemotaxis.

Switching direction in electrotaxis can be explained by the balance of multiple pathways acting in parallel to bias cell migration toward the cathode or anode as follows (Fig. 5). In this model, PI3Ks and cGMP mediate cathode-directed signaling, whereas the N-terminal domain of sGC mediates anode-directed signaling. In addition, an unidentified pathway X, responsible for anode-directed signaling, is included in the model because even under simultaneous inhibition of PI3Ks and GCase, cells can still exhibit anode-directed electrotaxis (Fig. 2). Furthermore, to explain the inhibitory effects of the catalytic domain of sGC on the N-terminal domain, we assumed that cGMP not only mediates cathode-directed signaling by GbpC activation but also suppresses anode-directed signaling mediated by the N-terminal domain. According to this assumption, the sGC-dependent signaling pathways can switch in response to intracellular cGMP levels. At a higher concentration of cGMP, cathode-directed signaling becomes dominant by both activation of GbpC-mediated cathode-directed signaling and suppression of N-terminal-domain-mediated, anode-directed signaling. On the other hand, at a lower concentration of cGMP, anode-directed signaling becomes dominant by both inhibition of GbpC and release of the N-terminal domain suppression. As shown in Fig. 4, sGC-GFP and sGCΔCat-GFP were localized dominantly to the pseudopod directed toward the cathode and the anode, respectively. These results suggest that sGC localization toward the cathode and the anode in electrotaxis is regulated by the catalytic domain and that the catalytic product cGMP works as a directional switcher in electrotaxis.

Based on this model, we estimated the relative contributions of 4 signaling pathways on the directedness of electrotaxis (Fig. S1). PI3Ks, GbpC, the N-terminal domain of sGC, and the

unidentified X pathway were estimated to have respective directedness values of 0.6, 0.25, −0.3, and −0.25 units in the absence of cAMP, where positive and negative values indicate directedness for migration toward the cathode and anode, respectively (Fig. S1*A*). In the presence of cAMP, the values are modulated because the enzymatic activities of PI3Ks and sGC are sensitive to cAMP stimulation (Fig. S1*B*) (18–21, 35). Simple summation of the directedness values estimated for the individual pathways can explain the obtained directedness in almost all experimental conditions (Table S2). Thus, the hypothetical model can explain migration direction in electrotaxis as a tug-of-war-like mechanism between multiple-signaling pathways. It would be worth exploring the involvement of other chemotactic signals such as Ras, TORC2, PLCγ, and PLA2 in directional control during electrotaxis (19–21, 36, 37). These studies would further contribute to an understanding of the molecular mechanisms involved in the coupling between gradient sensing and directional cell migration.

Materials and Methods

Cell Preparation and Electrotactic Assay. Ax2 cells (WT) and knockout cell lines were grown at 21 °C in HL5 medium supplemented with 5 ng/mL vitamin B12 and 100 ng/mL folic acid (23). Strains of *gc*-null and *gbpA*$^{-}$/*gbpB*$^{-}$ cells were obtained from the Dicty Stock Center and selected with 10 μg/mL blasticidin S. The *gbpC*-null strain was created in WT Ax3 background, similar to a previously described method using DH1 background (28), and selected with 10 μg/mL blasticidin S. *gc*-null/sGCΔCat-expressing sGC-D1106A in *gc*-null cells and *gc*-null/sGCΔN-expressing sGC with an N-terminal deletion of 877 aa in *gc*-null cells were selected with 10 μg/mL G418 (18, 33). KI mutant cells were grown on a 5LP plate (0.5% lactose/0.5% proteose peptone/1.5% agar) with *Escherichia coli* B/r at 21 °C (24).

Expression of sGC-GFP in *gc*-null cells has been previously described (35). For the expression of GbpC-GFP, the full *gbpC* ORF was amplified from cDNA by PCR and cloned in plasmid MB74-GFP, yielding a C-terminal GFP-fusion of GbpC, which was subsequently expressed in *gbpC*-null cells. $PH_{Akt/PKB}$ and PI3K2 were tagged with enhanced GFP. Cells expressing sGC-GFP, GbpC-GFP, PI3K2-GFP, and $PH_{Akt/PKB}$-GFP were selected with 20 μg/mL G418.

For electrotactic assays, cells were starved by a standard method (23). The starved cells were suspended in development buffer containing 10 mM Na/K PO_4, 2 mM $MgSO_4$, and 0.2 mM $CaCl_2$, (pH 6.5). In electrotactic assays for Ax2, *gbpA*$^{-}$/*gbpB*$^{-}$, *gc*-null, *gbpC*-null, *gc*-null/sGCΔN, and *gc*-null/sGCΔCat cells, 4 mM caffeine was added to inhibit adenylyl cyclase activity, which in turn reduced cell–cell interactions (38).

The construction of the chambers for electrotactic assays and dcEF application has been previously described (23). The cells in the chamber were observed with an Olympus IX-71 inverted microscope capable of producing phase contrast optics. Cell behavior was recorded with a cooled CCD camera (MicroMax; Princeton Instruments) and software (MetaMorph; Molecular Devices) in a personal computer. To trace cell trajectories, images were processed automatically by using lab-developed software. From the positional changes, motile properties such as directedness, migration velocity, path linearity, and asymmetric index were obtained by a previously reported method (23).

Fluorescence Imaging. To visualize GFP fused proteins, cells were examined through an inverted microscope (TE2000-PFS; Nikon) with an Apo TIRF 60×1.49 oil immersion lens. Confocal images were obtained by using a CSU10 scanner unit (Yokogawa) at an excitation wavelength of 488 nm from a DPSS laser (Sapphire 488–200 CDRH; Coherent) with an EM-CCD camera (iXon^{EM+} DU-897; Andor). A barrier filter was used to detect emissions of >522 nm. The image was captured with Andor IQ software.

ACKNOWLEDGMENTS. We thank all members of the T.Y. laboratory for discussions and technical assistance, Peter Karagiannis for reading the manuscript, and Y. Asano and T. Uyeda (National Institute of Advanced Industrial Science and Technology, Ibaraki, Japan) for the kind gift of $PH_{Akt/PKB}$-EGFP plasmid. M.J.S. is supported by a research fellowship of the Japan Society for the Promotion of Science. This study was supported by Leading Project Bio-Nano-Process of the Japanese Ministry of Education, Culture, Sports, Science and Technology and was supported in part by the Yuragi Project of the Japanese Ministry of Education, Culture, Sports, Science and Technology.

1. Bray D (2001) *Cell Movements: From Molecules to Motility*. (Garland, New York).
2. Song H, et al. (1998) Conversion of neuronal growth cone responses from repulsion to attraction by cyclic nucleotides. *Science* 281:1515–1518.
3. Nishiyama M, et al. (2003) Cyclic AMP/GMP-dependent modulation of Ca2+ channels sets the polarity of nerve growth-cone turning. *Nature* 423:990–995.
4. Keizer-Gunnink I, Kortholt A, Van Haastert PJ (2007) Chemoattractants and chemorepellents act by inducing opposite polarity in phospholipase C and PI3-kinase signaling. *J Cell Biol* 177:579–585.
5. Robinson KR (1985) The responses of cells to electrical fields: A review. *J Cell Biol* 101:2023–2027.
6. Nuccitelli R (2003) A role for endogenous electric fields in wound healing. *Curr Top Dev Biol* 58:1–26.
7. Mycielska ME, Djamgoz MB (2004) Cellular mechanisms of direct-current electric field effects: Galvanotaxis and metastatic disease. *J Cell Sci* 117:1631–1639.
8. McCaig CD, Rajnicek AM, Song B, Zhao M (2005) Controlling cell behavior electrically: Current views and future potential. *Physiol Rev* 85:943–978.
9. Lin F, et al. (2008) Lymphocyte electrotaxis in vitro and in vivo. *J Immunol* 181:2465–2471.
10. Li X, Kolega J (2002) Effects of direct current electric fields on cell migration and actin filament distribution in bovine vascular endothelial cells. *J Vasc Res* 39:391–404.
11. Zhao M, Bai H, Wang E, Forrester JV, McCaig CD (2004) Electrical stimulation directly induces pre-angiogenic responses in vascular endothelial cells by signaling through VEGF receptors. *J Cell Sci* 117:397–405.
12. Wang E, Zhao M, Forrester JV, McCaig CD (2003) Bi-directional migration of lens epithelial cells in a physiological electrical field. *Exp Eye Res* 76:29–37.
13. Segall JE, Gerisch G (1989) Genetic approaches to cytoskeleton function and the control of cell motility. *Curr Opin Cell Biol* 1:44–50.
14. Schleicher M, Noegel AA (1992) Dynamics of the Dictyostelium cytoskeleton during chemotaxis. *New Biol* 4:461–472.
15. Eichinger L, Lee SS, Schleicher M (1999) Dictyostelium as model system for studies of the actin cytoskeleton by molecular genetics. *Microsc Res Tech* 47:124–134.
16. Fukui Y (2002) Mechanistics of amoeboid locomotion: Signal to forces. *Cell Biol Int* 26:933–944.
17. Takagi H, Sato MJ, Yanagida T, Ueda M (2008) Functional analysis of spontaneous cell movement under different physiological conditions. *PLoS ONE* 3:e2648.
18. Veltman DM, Keizer-Gunnik I, Van Haastert PJ (2008) Four key signaling pathways mediating chemotaxis in Dictyostelium discoideum. *J Cell Biol* 180:747–753.
19. Kölsch V, Charest PG, Firtel RA (2008) The regulation of cell motility and chemotaxis by phospholipid signaling. *J Cell Sci* 121:551–559.
20. Janetopoulos C, Firtel RA (2008) Directional sensing during chemotaxis. *FEBS Lett* 582:2075–2085.
21. Kay RR, Langridge P, Traynor D, Hoeller O (2008) Changing directions in the study of chemotaxis. *Nat Rev Mol Cell Biol* 9:455–463.
22. Zhao M, Jin T, McCaig CD, Forrester JV, Devreotes PN (2002) Genetic analysis of the role of G protein-coupled receptor signaling in electrotaxis. *J Cell Biol* 157:921–927.
23. Sato MJ, et al. (2007) Input-output relationship in galvanotactic response of Dictyostelium cells. *BioSystems* 88:261–272.
24. Kuwayama H, Ishida S, Van Haastert PJ (1993) Non-chemotactic Dictyostelium discoideum mutants with altered cGMP signal transduction. *J Cell Biol* 123:1453–1462.
25. Liu G, Kuwayama H, Ishida S, Newell PC (1993) The role of cyclic GMP in regulating myosin during chemotaxis of Dictyostelium: Evidence from a mutant lacking the normal cyclic GMP response to cyclic AMP. *J Cell Sci* 106:591–595.
26. Kuwayama H, Viel GT, Ishida S, Van Haastert PJ (1995) Aberrant cGMP-binding activity in nonchemotactic Dictyostelium discoideum mutants. *Biochim Biophys Acta* 1268:214–220.
27. Roelofs J, Van Haastert PJ (2002) Characterization of two unusual guanylyl cyclases from dictyostelium. *J Biol Chem* 277:9167–9174.
28. Bosgraaf L, et al. (2002) A novel cGMP signalling pathway mediating myosin phosphorylation and chemotaxis in Dictyostelium. *EMBO J* 21:4560–4570.
29. Bosgraaf L, Van Haastert PJ (2002) A model for cGMP signal transduction in Dictyostelium in perspective of 25 years of cGMP research. *Muscle Res Cell Motil* 23:781–791.
30. Zhao M, et al. (2006) Electrical signals control wound healing through phosphatidylinositol-3-OH kinase-gamma and PTEN. *Nature* 442:457–460.
31. Loovers HM, et al. (2006) Distinct roles of PI(3,4,5)P3 during chemoattractant signaling in Dictyostelium: A quantitative in vivo analysis by inhibition of PI3-kinase. *Mol Biol Cell* 17:1503–1513.
32. Sasaki AT, et al. (2007) G protein-independent Ras/PI3K/F-actin circuit regulates basic cell motility. *J Cell Biol* 178:185–191.
33. Veltman DM, Van Haastert PJ (2006) Guanylyl cyclase protein and cGMP product independently control front and back of chemotaxing Dictyostelium cells. *Mol Biol Cell* 17:3921–3929.
34. Sebestikova L, Slamova E, Sevcikova H (2005) Control of wave propagation in a biological excitable medium by an external electric field. *Biophys Chem* 113:269–274.
35. Veltman DM, Roelofs J, Engel R, Visser AJ, Van Haastert PJ (2005) Activation of soluble guanylyl cyclase at the leading edge during Dictyostelium chemotaxis. *Mol Biol Cell* 16:976–983.
36. Van Haastert PJ, Keizer-Gunnink I, Kortholt A (2007) Essential role of PI3-kinase and phospholipase A2 in Dictyostelium discoideum chemotaxis. *J Cell Biol* 177:809–816.
37. Chen L, et al. (2007) PLA2 and PI3K/PTEN pathways act in parallel to mediate chemotaxis. *Dev Cell* 12:603–614.
38. Brenner M, Thoms SD (1984) Caffeine blocks activation of cyclic AMP synthesis in Dictyostelium discoideum. *Dev Biol* 101:136–146.